

Suppressing Fermi acceleration in a time-dependent stadium billiard with scaling analysis

André L. P. Livorati and Edson D. Leonel

*DEMAC – Instituto de Geociências e Ciências Exatas – Universidade Estadual Paulista
Av.24A, 1515 – Bela Vista – CEP: 13506-700 – Rio Claro – SP – Brazil*

The dynamics of a dissipative time-dependent stadium-like billiard are studied by a four dimensional nonlinear mapping. The dissipation was introduced via inelastic collision between the particle and the moving wall. We have shown that, for different combinations of initial velocity and the damping coefficient, the particle dynamics converge to different sinks and different plateaus for a high number of collisions. We also characterized a phase transition, through scaling arguments, from limited to unlimited energy growth, when the damping coefficient tends to unity.

PACS numbers: 05.45.Pq, 05.45.Tp

I. INTRODUCTION

Billiard problems are well known in the literature as problems involving particles (billiard balls), interacting, or not with themselves, suffering elastic collisions inside a closed domain. These elastic collisions obeys the specular reflection law, i. e., while the tangent component is preserved, the normal one changes its sign at the collision point, and the particle is reflected elastically [1]. Thanks to the papers of Sinai [2–4] and Bunimovich [5–7], who were the pioneers in the study of billiards, we have today the necessary mathematical formulation for a some new rigorous analysis. Nowadays, billiard problems can be found in several fields of physics and other sciences, like optics [8–10], quantum dots [11], microwaves [12], astronomy [13], laser dynamics [14], etc.

When the billiard boundaries are time-dependent, i. e., $\partial Q = \partial Q(t)$, we may find an interesting phenomenon, called Fermi acceleration (FA). Introduced for the first time in 1949 by the Italian physicist Enrico Fermi [15], FA is basically the unlimited energy growth for a point-particle suffering elastic collisions with a time-dependent boundary. When we considered two-dimensional billiards, this phenomenon has already been studied [16–23, 35]. One of the main questions about FA in perturbed systems is whether the energy of the particle can grow to infinity. This answer is far away from trivial and depends on the kind of perturbation as well the billiard boundaries geometry. The Loskutov-Ryabov-Aikinshin (LRA) conjecture [21], presents a mechanism that produces FA. If a billiard, in the static boundary case, has any chaotic component in the phase space, the introduction of the time perturbation is sufficient condition for the system presents FA. However, F. Lenz et. al [22] shown that even for an elliptical billiard, which has regular dynamics in the static boundary case, presents FA, when the time perturbation is introduced. In this case, FA is produced by orbits that cross in the phase space the region of the stochastic layer, changing their dynamics from libration to rotator [1], or vice-versa. This crossing behavior is the FA production mechanism.

Leonel and Bunimovich [23], extended the LRA conjecture, showing that only the presence of heteroclinic orbits are sufficient condition for the billiard exhibits FA. The introduction of dissipation, is sufficient condition to suppress FA. Indeed, it has already been observed in other systems where dissipation can be introduced via inelastic collisions with the moving boundary [24–29], by a drag force [30, 31], or even by kinetic friction [32]. This last one, depending on kind of the time perturbation introduced on the boundary, can even produce FA [32].

Often, the dynamics of the system depends on the control parameters. Particularly, such parameters can control the intensity of the non-linearity of the system and, as they change, average quantities of the dynamics can experience subtle modifications, therefore characterizing a phase transition [33]. Many of these transitions can be described by using scaling arguments where critical exponents play an important role in the description of the average properties [20, 27, 29, 32, 34].

This paper is organized as follows: In Sec.II a dissipative time-dependent stadium billiard is studied, where dissipation is introduced via inelastic collisions. The dynamics are described by a four nonlinear mapping, and we considered the simplified approach, where the boundary is fixed, but when the particle collides with it, they exchange momentum as if the boundary were moving. In Sec.III, we show how the introduction of dissipation via inelastic collisions can suppress the unlimited energy growth of FA, and we also show some numerical results, where we observe that the combination of the control parameters influences on the dynamics of the particle. The scaling analysis for the average velocity as function of the control parameters initial velocity and the damping coefficient are found in Sec.IV. Finally, Sec.V we draw some final remarks and conclusions.

II. THE MODEL AND THE MAPPING

We considered the dynamics of a point particle suffering inelastic collisions inside a time-dependent stadium

billiard. The inelastic collisions are introduced by two distinct damping coefficients γ and β , where γ is the normal component damping coefficient and β is the coefficient of the tangent one, and both $\in [0, 1]$ (See Ref.[28]). If $\gamma = \beta = 1$, we recovered the conservative case, where the system presents FA [35]. In order to describe the particle dynamics, we studied the system in two different cases: (i) successive collisions, and (ii) indirect collisions. In (i) the particle suffers successive collisions with the same focusing component, and in (ii) after suffer a collision with the opposite one. The time dependence in the boundary is introduced by $R(t) = R_0 + r \sin(wt)$, where $R_0 \gg r$. The boundary velocity equation is obtained of $\dot{R}(t)$, so

$$\dot{R}(t) = B(t) = B_0 \cos(wt) , \quad (1)$$

where $B_0 = rw$ is the amplitude of oscillation of the moving boundary and w is the frequency of oscillation. It is always good to remember that we are adopting a simplified approach, where the boundary is fixed, but it exchange momentum with the particle as if it was moving. In order to simplify our numerical analysis, for future calculations we considered $w = 1$.

The dynamics variables are (α, φ, t, V) , where α is the angle between the trajectory of the particle and the normal line at the collision point, and φ is the angle between the the normal line at the collision point and the vertical line in the symmetry axis. We assume that V_n is the particle velocity and t_n is the time in the instant of the n^{th} collision, and at the initial time $t_0 = 0$, the particle belongs to the focusing boundary and the velocity vector directs towards to the billiard table. Just for notation, all variables with a (*) index, are measured just before the collision point. Figure 1 shows an illustration of a trajectory with successive collisions, where $R = a^2 + 4b^2/8b$ and $\Phi = \arcsin(a/2R)$. The geometric control parameters a , b and l are expressed in Fig.2, and in particular, if $a = 2b$ we recover the original stadium billiard [5]. For successive collision happen, it is necessary that $|\varphi_{n+1}| \leq \Phi$, and according to Fig.1 and the specular reflection law, we may obtain these relations

$$\begin{aligned} \alpha_{n+1}^* &= \alpha_n \\ \varphi_{n+1} &= \varphi_n + \pi - 2\alpha_n \pmod{2\pi} . \\ t_{n+1} &= t_n + \frac{2R \cos(\alpha_n)}{V_n} . \end{aligned} \quad (2)$$

Now, let us focus in the case of indirect collisions. For this case, it is necessary that $|\varphi_{n+1}| > \Phi$. In order to describe in an appropriate way the dynamics, the unfolding method [1] is used, besides two auxiliaries variables, ψ which is the angle between the trajectory and the vertical line at the collision point and x_n which is the projection of the particle position under the horizontal axis.

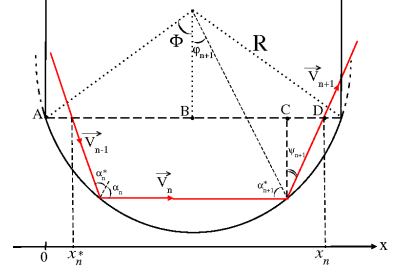


FIG. 1: (color online) *Dynamical variables and a trajectory with successive collisions.*

Looking at the Fig.1 we can geometrically obtain the value of the angle $\psi_n = \alpha_n - \varphi_n$. We also can see that x_n is the sum of the line segments $\overline{AB} + \overline{BC} + \overline{CD}$. Taking into account the value of ψ_n , and, after some algebra, we obtain $x_n = \frac{R}{\cos(\psi_n)} [\sin(\alpha_n) + \sin(\Phi - \psi_n)]$. The recurrence relation between x_n and x_{n+1} is given by the unfolding method, described in Fig.2, as $x_{n+1} = x_n + l \tan(\psi_n)$.

Now, let us find the equations for the angular dynamical variables and time. If we invert the particle motion, i. e., considering the reverse direction of the billiard particle, then the expression that furnishes the value of x_n is also inverted and the angle α_n , became α_n^* . Resolving it with respect to α_n^* , taking into account that this angle is changed in the opposite direction than α_n , and the angle φ_n should have the reversed sign, we now can get the value of the incident angle α_n^* , that will become α_{n+1}^* when we re-inverted the particle motion. The values of φ_{n+1} and the time t_{n+1} can be obtained by easy geometrical considerations on Fig.2. Thus, we obtain the mapping for the case where indirect collisions happen, as

$$\begin{aligned} \alpha_{n+1}^* &= \arcsin[\sin(\psi_n + \Phi) - x_{n+1} \cos(\psi_n)/R] . \\ \varphi_{n+1} &= \psi_n - \alpha_{n+1}^* . \\ t_{n+1} &= t_n + \frac{R[\cos(\varphi_n) + \cos(\varphi_{n+1}) - 2 \cos(\Phi)] + l}{V_n \cos(\psi_n)} . \end{aligned} \quad (3)$$

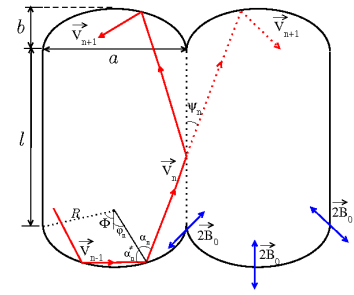


FIG. 2: (color online) *The unfolding method, the geometrical control parameters and a trajectory with indirect collisions.*

For both cases, i. e., successive and indirect collisions,

the recurrence relations of the velocity and the angle α_n are the same. Let us now focus in how to obtain them. Expressing the vectorial components for the velocity we may found

$$\begin{aligned}\vec{v}_n \cdot \vec{T}_n &= -v_n \cos(\alpha_n^*) . \\ \vec{v}_n \cdot \vec{N}_n &= v_n \sin(\alpha_n^*) .\end{aligned}\quad (4)$$

Making a change from inertial to non inertial referential, we can express the particle velocity as

$$\vec{V}_p = \vec{v}_w + \vec{v}'_p , \quad (5)$$

where \vec{V}_p and \vec{v}_w are respectively the particle velocity and the moving wall velocity in the inertial referential, and \vec{v}'_p is the particle velocity in the non inertial referential. The reflection laws for the dissipative case are expressed by

$$\begin{aligned}\vec{V}'_{n+1} \cdot \vec{T}_{n+1} &= \beta \vec{V}'_n \cdot \vec{T}_n , \\ \vec{V}'_{n+1} \cdot \vec{N}_{n+1} &= -\gamma \vec{V}'_n \cdot \vec{N}_n ,\end{aligned}\quad (6)$$

where β and γ are respectively the tangent and the normal damping coefficients.

Combining Eqs.(5) and (6), and also coming back to the inertial referential, we may found

$$\begin{aligned}\vec{V}_{n+1} \cdot \vec{T}_{n+1} &= \beta \vec{V}_n \cdot \vec{T}_{n+1} + (1 - \beta) \vec{B}(t_{n+1}) \cdot \vec{T}_{n+1} , \\ \vec{V}_{n+1} \cdot \vec{N}_{n+1} &= -\gamma \vec{V}_n \cdot \vec{N}_{n+1} + (1 + \gamma) \vec{B}(t_{n+1}) \cdot \vec{N}_{n+1} ,\end{aligned}\quad (7)$$

where $B(t_{n+1})$ is expressed by Eq.(1) evaluated at the time t_{n+1} .

Now, we can write the recurrence relation for the particle velocity as

$$|\vec{V}_{n+1}| = \sqrt{(\vec{V}_{n+1} \cdot \vec{T}_{n+1})^2 + (\vec{V}_{n+1} \cdot \vec{N}_{n+1})^2} . \quad (8)$$

According to the reflection law [1], we may found the relation between the angles α_n and α_n^* , through the velocity vectors \vec{V}_{n+1} and \vec{V}_n . Such relation is given by

$$\alpha_n = \arcsin \left(\frac{|\vec{V}_n|}{|\vec{V}_{n+1}|} \sin(\alpha_n^*) \right) . \quad (9)$$

III. SUPPRESSING FERMI ACCELERATION

In this section, we will study how the properties of the average velocity as function of the number of collision

with the moving wall change as we range the control parameters of initial velocity V_0 and the damping coefficient of the normal component γ . It is important to clarify that the damping coefficient of the tangent component β was fixed in $\beta = 1$, and the collisions with the line segments, considering the unfolding method, are completely elastic in both tangent and normal components.

The average velocity is defined by

$$\bar{V} = \frac{1}{M} \sum_{j=1}^n V_j(n, V_0, \gamma) , \quad (10)$$

where M is an ensemble of 5000 different initial conditions (α, φ) and V_j is expressed by

$$V(n, V_0, \gamma) = \frac{1}{n} \sum_{i=1}^n V_i , \quad (11)$$

where n is the number of collisions with the moving wall.

We evaluated the dynamics in two different ways. In the first one, the initial velocity was fixed in $V_0 = 100$ and we ranged the damping coefficient γ , and in the second one, we ranged the initial velocity and the value of the damping coefficient was fixed in $\gamma = 0.999$. Figures 3 and 4 shows the evolutions of these dynamics iterated up to 10^9 collisions with the moving wall. As we already known [27?–29], inelastic collisions should suppress the phenomenon of FA, and indeed, when we introduce this kind of dissipation, the unlimited energy growth is no longer observed. It is important to us to clarify that in the whole numerical analysis of this paper, the geometric control parameters were fixed as $a = 0.5$, $b = 0.01$ and $l = 1$ and the amplitude of oscillation of the moving wall was also fixed as $B_0 = 0.01$.

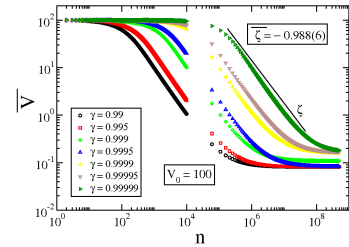


FIG. 3: (color online) \bar{V} curves as function of n with fixed initial velocity in $V_0 = 100$ and the damping coefficient γ ranging as labeled in the figure.

Analyzing both Figs.3 and 4, one can see that they present a similar initial behavior. The \bar{V} curves start in a constant regime of each initial velocity, and then, depending on the value of the damping coefficient, they experience a crossover (n_x), and start to decay according a power law, with exponent $\zeta \approx -1$. However, after the power law decay, for a high number of collisions, the \bar{V}

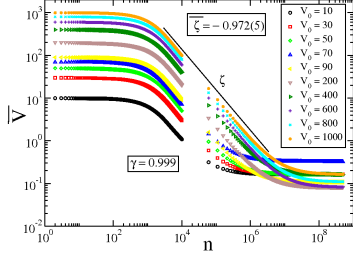


FIG. 4: (color online) \bar{V} curves as function of n with damping coefficient fixed $\gamma = 0.999$ and the initial velocity ranging as labeled in the figure.

curves saturates in different plateaus, as we range the control parameters V_0 and γ .

A. Dependence on γ and V_0

In order to understand why the \bar{V} curves saturate in different plateaus when we range the control parameters (V_0, γ) , we constructed a phase space in the variables (ξ, ψ) , where $\xi = 0.5 + x_n/a$. So, we can compare with the conservative case [21, 35] and see what happen with the particle dynamics. Figure 5 shows a phase space (ξ, ψ) for 25 different pairs of initial conditions (α, φ) evaluated up to 10^8 collisions with the moving wall. As one can see, when dissipation is introduced, the invariant curves are destroyed and the fixed points became sinks [36], and depending on the combinations of the control parameters (V_0, γ) , the particle converges to different sinks, suppressing the phenomenon the unlimited energy growth which characterizes FA.

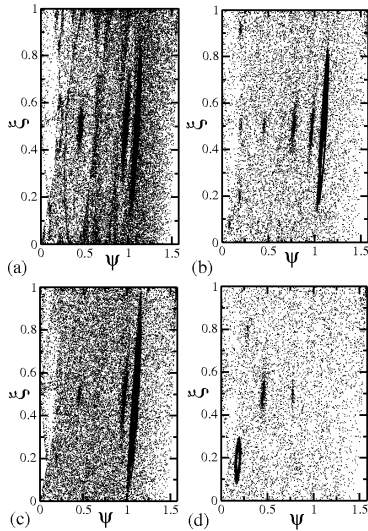


FIG. 5: Phase space (ξ, ψ) . The control parameters used were (a) $V_0 = 100$, $\gamma = 0.9999$; (b) $V_0 = 100$, $\gamma = 0.999$; (c) $V_0 = 10$, $\gamma = 0.999$ and (d) $V_0 = 1000$, $\gamma = 0.99$.

In order show how this convergence to sinks influences the velocity of the particle, we show in Fig.6 a zoom in the region of the low velocities in a phase space with the variables velocity and time taken ($\text{mod } 2\pi$), for the same combination of control parameters used on the construction of the phase space of the Fig.5 and the same 25 initial conditions evaluated up to 10^8 collisions with the moving wall. Analyzing Fig.6 we can clearly see, that each combination of (V_0, γ) leads to a different region of attraction of the particle velocity by the sinks, leading to a velocity decreasing. We believe that, this different sinks are the responsible for the different plateaus of the \bar{V} saturation in the regime of a high number of collisions.

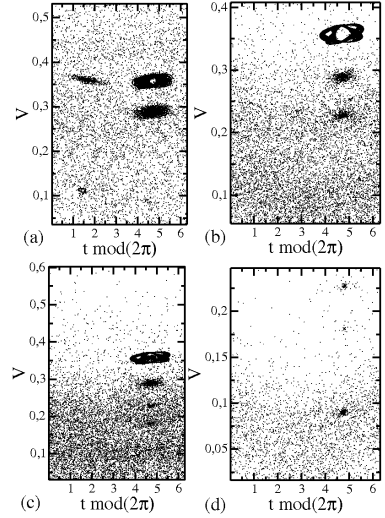


FIG. 6: Phase space $(V, t \text{ mod}(2\pi))$. The control parameters used were (a) $V_0 = 100$, $\gamma = 0.9999$; (b) $V_0 = 100$, $\gamma = 0.999$; (c) $V_0 = 10$, $\gamma = 0.999$ and (d) $V_0 = 1000$, $\gamma = 0.99$.

IV. SCALING PROPERTIES

Analyzing the dynamics of \bar{V} discussed in Sec.III, we can see that the curves of \bar{V} obeys, in the initial number of collisions with the moving wall, a similar behavior. They start in a constant regime of initial velocity, and then they experience a first crossover (n_x) and start decaying according a power law with exponent $\zeta \approx -1$. This initial behavior, does not change when we range the control parameters V_0 and γ . So, in order to describe in a statistical way the initial regime of the curves of \bar{V} we propose some scaling hypothesis

(i) $\bar{V} \propto V_0^\alpha$, for $n \ll n_x$, where α is a critical exponent;

(ii) $\bar{V} \propto \left(\frac{n}{V_0}\right)^\zeta$, for $n \gg n_x$, where $\zeta \approx -1$ is the power law decaying exponent;

(iii) $\left(\frac{n_x}{V_0}\right) \propto V_0^{z_1}(1-\gamma)^{z_2}$, where z_1 e z_2 are dynamical exponents.

On the scaling hypothesis (iii) we considered $(1-\gamma)$ instead of γ , because we want to bring the criticality of the phase transition from limited to unlimited energy growth to $(1-\gamma) \rightarrow 0$, and also we considered that the proportional relation between V_0 and n_x , must obey the power law $n_x/V_0 \propto V_0^{z_1}$, because as one can see in Fig.4 the collision crossover number (n_x) is the almost the same, does not matter the value of the initial velocity. So, it seems that the best variable to be analyzed is (n/V_0) instead of only n . In Figure 7 we show the curves of \bar{V} after a transformation to the best variable (n/V_0) . All the \bar{V} curves starts in a constant regime of initial velocity, and then decay together in power law exponent $\zeta \approx -1$.

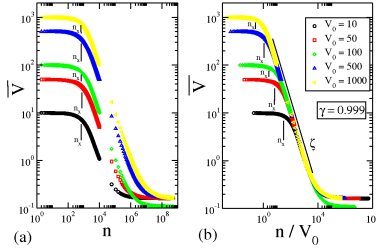


FIG. 7: (color online) *Transformation to the best variable.* In (a) curves of \bar{V} as function of n , and in (b) the same curves of (a) as function of n/V_0 . The dissipation control parameter was fixed in $\gamma = 0.999$.

Considering that in all curves of \bar{V} showed in Figs.3, 4 and 7, the dynamics start in a constant regime of initial velocity, we can easily obtain the critical exponent of the scaling hypothesis (i) as $\alpha = 1$. The dynamics exponents z_1 and z_2 are obtained respectively by a power law fitting according to $(n_x/V_0) \times V_0$ and $(n_x/V_0) \times (1-\gamma)$. Figure 8 furnishes the numerical values of the dynamical exponents as $z_1 = -0.99(1)$ and $z_2 = -0.968(1)$.

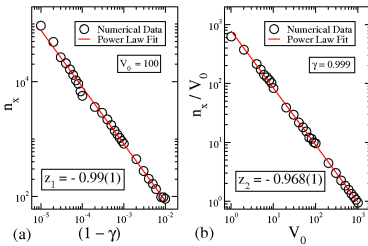


FIG. 8: (color online) In (a) we have the power law fit of $n_x/V_0 \times V_0$, where $\gamma = 0.999$ was fixed; and in (b) we show the power law fitting of $n_x \times (1-\gamma)$, where $V_0 = 100$ was constant. Both fittings (a) and (b), furnishes the values of the dynamical exponents as $z_1 = -0.99(1)$ and $z_2 = -0.968(1)$.

Now, let us now focus in describe the initial dynamical regime of the \bar{V} curves in a statistical way. We propose a generic homogeneous function for the behavior of \bar{V} as

$$\bar{V}(n/V_0, V_0(1-\gamma)) = l(l^a n/V_0, l^b V_0(1-\gamma)) , \quad (12)$$

where l is a scaling factor and a and b are scaling exponents.

By taking $l^a n/V_0$ constant, we have

$$l = \left(\frac{n}{V_0}\right)^{-\frac{1}{a}} . \quad (13)$$

Replacing Eq.(13) in Eq.(12), we obtain

$$\bar{V}(n/V_0, V_0(1-\gamma)) = V_0^{-\frac{1}{a}} \bar{V}_1(1, l^{-\frac{b}{a}} V_0(1-\gamma)) . \quad (14)$$

Comparing Eq.(14) with the scaling hypothesis (ii), \bar{V}_1 is assumed to be constant for $n \gg n_x$, and how we already known the value of $\zeta \approx -1$, so

$$\zeta = -\frac{1}{a} \Rightarrow a = 1 . \quad (15)$$

Choosing now $l^b V_0(1-\gamma)$ constant, we found

$$l = (V_0(1-\gamma))^{-\frac{1}{b}} . \quad (16)$$

Replacing Eq.(16) in Eq.(12), we obtain

$$\bar{V}(n/V_0, V_0(1-\gamma)) = V_0(1-\gamma)^{-\frac{1}{b}} \bar{V}_2(l^{-\frac{a}{b}} n/V_0, 1) . \quad (17)$$

Comparing Eq.(17) with the scaling hypothesis (i), \bar{V}_2 is also assumed to be constant for $n \ll n_x$ and how we already know the value of $\alpha = 1$, and once the initial regime of the dynamics does not suffers influence of the dissipation control parameter, the term $(1-\gamma)$, is encompassed by the proportionality constant \bar{V}_2 , so we have

$$\alpha = -\frac{1}{b} \Rightarrow b = -1 . \quad (18)$$

By taking the crossover choice and equaling Eqs.(13) and (16), we found

$$\left(\frac{n}{V_0}\right)^{-\frac{1}{a}} = (V_0(1-\gamma))^{-\frac{1}{b}} . \quad (19)$$

Raising Eq.(19) to the power of $(-a)$, we obtain

$$\left(\frac{n}{V_0}\right) = (V_0(1-\gamma))^{\frac{a}{b}} . \quad (20)$$

Comparing Eq.(20) with the scaling hypothesis (iii), and considering the results furnished by Fig.8, we found the following expressions

$$\frac{a}{b} = z_1 = z_2 \quad , \quad \frac{\alpha}{\zeta} = z_1 = z_2 \quad . \quad (21)$$

Once known the scaling law, we now can collapse all the curves of \bar{V} in a plot that describes the behavior of \bar{V} for a initial number of collisions as function of the control parameters initial velocity and dissipation. Figure 9 shows perfectly this collapse, where all the curves of Fig.9(a) are collapsed in Fig.9(b) for short times.

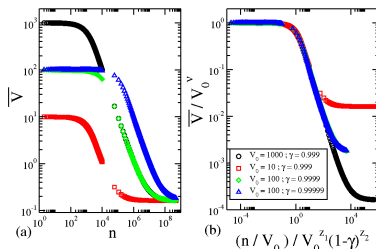


FIG. 9: (color online) In (a) we show the behavior of some curves of \bar{V} , and in (b) we have the collapse of all (a) curves into a single and universal plot for short times.

V. CONCLUSIONS

To conclude, we considered a time-dependent stadium-like billiard with dissipation introduced via inelastic collisions. A new recurrence relation for the velocity of the particle was found, considering the dissipation effects. With the introduction of the dissipation, the fixed points, said elliptic, became sinks, and the particle does not experience the FA phenomenon. We ranged the control parameters of initial velocity and dissipation, and observed a decreasing on the curves of \bar{V} according a power law decay with exponent $\zeta \approx -1$. We described the average velocity decaying through scaling analysis, besides, we characterized a phase transition from limited energy growth to unlimited energy growth when the damping coefficient $\gamma \rightarrow 1$, confirming that the phenomenon of FA is not structurally stable.

ACKNOWLEDGES

ALPL thanks to FAPESP for the financial support. EDL thanks to FAPESP, CNPq, Capes and Fundunesp.

-
- [1] N. Chernov and R. Markarian, *Chaotic Billiards*. (American Mathematical Society, Vol. 127, 2006).
 - [2] Y. G. Sinai, Math. Dokl., **4**, 1818 (1963).
 - [3] Y. G. Sinai, Russ. Math. Surveys, **25**, 137 (1970).
 - [4] Y. G. Sinai, Russ. Math. Surveys, **25**, 141 (1970).
 - [5] L. A. Bunimovich, Funct. Anal. Appl., **8**, 254 (1974).
 - [6] L. A. Bunimovich, Commun. Math. Phys., **65**, 295 (1979).
 - [7] L. A. Bunimovich and Y. G. Sinai, Commun. Math. Phys., **78**, 479 (1981).
 - [8] N. Friedman *et al.*, Phys. Rev. Lett., **86**, 1518 (2001).
 - [9] M. F. Andersen *et al.*, Phys. Rev. A, **69**, 63413 (2004).
 - [10] M. F. Andersen *et al.*, Phys. Rev. Lett., **97**, 104102 (2006).
 - [11] H. J. Stokmann, *Quantum Chaos: An Introduction*. Cambridge University Press - 1999.
 - [12] C. M. Marcus *et al.*, Phys. Rev. Lett., **69**, 506 (1992).
 - [13] P. Fré, A. S. Sorin, J. High Energy Phys., **3**, 1 (2010).
 - [14] A. D. Stone, Nature, **465**, 696 (2010).
 - [15] E. Fermi. Phys. Rev., **75**, 1169 (1949).
 - [16] E. D. Leonel, D. F. M. Oliveira and A. Loskutov, Chaos, **19**, 033142 (2009).
 - [17] D. F. M. Oliveira and E. D. Leonel, Commun. Nonlinear Sci. and Numer. Simulat., **15**, 1092 (2010).
 - [18] F. Lenz *et al.*, New J. Phys., **11**, 083035 (2009).
 - [19] A. K. Karlis *et al.*, Phys. Rev. Lett., **97**, 194102 (2007).
 - [20] E. D. Leonel, Phys. Rev. Lett., **98**, 114102 (2007).
 - [21] A. Loskutov, A. B. Ryabov and L. G. Akinshin, J. Phys. A, **33**, 7973 (2000).
 - [22] F. Lenz, F. K. Diakonov and P. Schemelcher, Phys. Rev. Lett., **100**, 014103 (2008).
 - [23] E. D. Leonel and L. Bunimovich, Phys. Rev. Lett., **104**, 224101 (2010).
 - [24] E. D. Leonel, J. K. Leal da Silva and P. V. E. McClintock, Phys. Rev. Lett., **93**, 014101 (2004).
 - [25] E. D. Leonel and P. V. E. McClintock, J. Phys. A, **38**, 823 (2005).
 - [26] E. D. Leonel and A. L. P. Livorati, Physica. A, **387**, 1155 (2008).
 - [27] A. L. P. Livorati, D. G. Ladeira and E. D. Leonel, Phys. Rev. E, **78**, 056205 (2008).
 - [28] D. F. M. Oliveira and E. D. Leonel, Physica A, **389**, 1009 (2010).
 - [29] D. F. M. Oliveira, J. Vollmer and E. D. Leonel, Physica D, **240**, 389 (2011).
 - [30] F. A. de Souza, L. E. A. Simões, M. R. da Silva, E. D. Leonel, Mathematical Problems in Engineering, vol. 2009, Article ID 409857 (2009).
 - [31] E. D. Leonel and L. Bunimovich, Phys. Rev. E, **81**, (2010).
 - [32] D. G. Ladeira, E. D. Leonel, Phys. Rev. E, **81**, 036216 (2010).
 - [33] R. K. Pathria, *Statistical Mechanics*, Elsevier – Burlington 2008.
 - [34] J. A. de Oliveira, R. A. Bizão and E. D. Leonel, Phys. Rev. E, **81**, (2010).
 - [35] A. B. Ryabov and A. Loskutov, J. Phys. A, **43**, (2010).
 - [36] A. J. Lichtenberg, M.A. Lieberman, *Regular and Chaotic*

Dynamics. Appl. Math. Sci. 38, Springer Verlag, New York, 1992.